SUPPORTING MATERIALS

Control of a Nanoscopic-to-Macroscopic Transition: Modulated Phases in 4-Component DSPC/DOPC/POPC/chol Giant Unilamellar Vesicles

Tatyana M. Konyakhina, [†Δ] Shih Lin Goh, [†Δ] Jonathan Amazon, [†] Frederick A. Heberle, [‡] Jing Wu, [§] and Gerald W. Feigenson[†]*

MATERIALS

Phospholipids were purchased from Avanti Polar Lipids (Alabaster, AL), and cholesterol was from Nu Chek Prep (Elysian, MN). Fluorescent dyes C12:0-DiI (1,1′-didodecyl-3,3,3′,3′-tetramethylindocarbocyanine perchlorate) and BoDIPY-PC (2-(4,4-difluoro-5,7-dimethyl-4-bora-3a,4a-diaza-s-indacene-3-pentanoyl)-1-hexadecanoyl-sn-glycero-3-phosphocholine) were from Invitrogen (Carlsbad, CA). Concentrations of phospholipid stocks were determined to <1% error with inorganic phosphate assay, and purity checked with thin layer chromatography in 65:25:4= chloroform/methanol/water solvent (1). Cholesterol at defined concentration was prepared by standard gravimetric procedures. Fluorescent dye concentrations were determined using absorption spectroscopy on an HP 8452A spectrophotometer (Hewlett-Packard, Palo Alto, CA).

SAMPLE PREPARATION AND MICROSCOPY

Giant unilamellar vesicles (GUVs) were prepared using a modified electroformation procedure as described in (2). GUVs were swelled at 55°C in 100 mM sucrose, and cooled to room temperature (23°C) over 10 hours. For 2-photon, confocal, and most wide-field fluorescence microscopy experiments, GUVs were diluted into 100 mM glucose before imaging. The difference in solution density allows vesicles to settle more efficiently and also creates a sufficient refractive index difference to enable locating and focusing on GUVs without intense illumination (1,3). For DIC microscopy, the internal and external media were kept identical (100 mM sucrose) to avoid mismatch in buffer refractive indices that might distort DIC imaging.

Wide-field microscopy was performed on the Nikon Diaphot-TMD and Nikon Ti-E Perfect Focus (Micro Video Instruments Inc., Avon, MA and Rochester, NY) inverted microscopes at 23°C using 60X 1.4NA oil immersion objectives. GUVs were labeled with C12:0-DiI at 0.02 mol%; the dye partitions preferentially into the Ld-phase. Controls for light-induced artifacts included samples with 0.014 and 0.01 mol % C12:0-DiI. To minimize light-induced artifacts, we used a combination of methods including lowering exposure time (down to 10-20 ms), using neutral density filters, and in particular, locating GUVs with transmitted light or DIC prior to exposure to the intense illumination needed for fluorescence imaging. Images were taken with a Photometrics charge-coupled device camera CoolSNAP$_{HQ2}$ (Tucson, Arizona) on the Diaphot-TMD, and with a DR328G Andor Clara Interline Camera (MVI Inc., Avon, MA and Rochester, NY) on the Ti-E. C12:0-DiI was imaged with 535-550 nm excitation and 565-610 nm emission on the Diaphot-TMD; 528-553 nm excitation and 590-650 nm emission on the Ti-E. Images were contrast-enhanced and analyzed with NIS Elements Basic Research Software (MVI, Inc.). Confocal imaging was performed on an inverted Zeiss 710 confocal microscope at 23°C using a

63X 1.4NA oil immersion objective. Confocal laser excitation was 561 nm (10.0 %) with pinhole 98 μm, and images collected at 564 – 684 nm. Confocal images were analyzed with Zeiss ZEN software. Two-photon microscopy was performed on home-built apparatus based on an inverted Zeiss Axiovert 35 microscope at 23°C using a 60X 1.2NA water immersion objective. Images were collected using a Hamamatsu HC125-02 Bialkali photomultiplier tube (Hamamatsu Corp., Middlesex, NJ). GUVs were labeled with 0.02 mol% BoDIPY-PC, which partitions preferentially into the Ld-phase. The excitation wavelength was 960 nm. Images were contrast-enhanced, and Z-projection image stacks prepared in Image J.

THEORY

The Landau-Ginzburg energy functional is a widely applicable phenomenological description of phase separation in field theory models (4). For our approach we modeled the local phase as a scalar field (order parameter) on the 2D plane with toroidal boundary conditions. The order parameter varies continuously on [−1,1], where (−1) represents Ld and (+1) represents Lo:

$$F = \iint [-B\phi^2(r) + \frac{B}{2}\phi^4(r) + \frac{K}{2}|\nabla\phi(r)|^2 + Q\mu(r)D[\mu](r)]\, dA \qquad \text{(S1)}$$

where ϕ is the order parameter at position r, B defines the free energy scale of the phase separation, μ is the local area density of molecular dipoles, D[μ](r) is the electric field normal to the membrane, K is proportional to line tension, and Q is the coupling coefficient for the field. Normally the quadratic and quartic couplings are independent; here they are fixed to ensure that the energy minima always occur at (±)1. The amount of each phase is fixed by constraining the order parameter to be conserved. We specify the amount of each phase by P, defined as the area fraction of Lo:

$$P = \frac{1}{2\mathrm{A_{Tot}}}\left[\iint \phi(r)\ dA\right] + \frac{1}{2} \qquad \text{(S2)}$$

where A_{Tot} is the total simulation area. The long range field term is computed as a convolution of the dipole density with the point source field (which goes as $1/r^3$).

$$\mu(r) = \left(\frac{\mu_o - \mu_d}{2}\right)\phi(r) + \left(\frac{\mu_o + \mu_d}{2}\right) \qquad \text{(S3)}$$

$$D[\mu](r) = \int \frac{\mu(r')}{|r - r'|^3}\, dA' \qquad \text{(S4)}$$

where μ_o and μ_d are the field source densities in the Lo and Ld phases, respectively. The order parameter is discretized and shuffled about the plane using a Monte Carlo/Metropolis algorithm to arrive at a minimal energy configuration. Competition between line tension (K) and the repulsive field term (Q) drives the system to reach equilibrium patterns approximating the

experimental observations. The field we studied here is modeled after electrostatic dipole-dipole interactions. Using electrostatics as the dispersive term does not take into account the effects of salt screening or the large dielectric mismatch from the interior/exterior of the membrane. To check the physicality of long range dipole interactions in bilayer membranes we solved for the electrostatic potential in and around a bilayer submerged in an ionic solution using the Poisson-Boltzmann equation (5)**:**

$$\nabla \cdot [\epsilon(r)\nabla V(r)] = \epsilon(r)\kappa^2(r)V(r) - \rho(r) \quad \text{(S5)}$$

where κ(r) is the inverse Debye length, ε(r) is the local dielectric, V(r) is the electrostatic potential, and ρ(r) is the charge density. Equation S5 was solved using an iterative relaxation method for a cylindrically symmetric charge distribution of two thin discs located at the headgroup/water interface and the headgroup/acyl chain interface to mimic an array of dipoles normal to the membrane. The dielectric is varied smoothly from the low dielectric in the chain region to the high dielectric of the water. κ varied discontinuously from zero inside the bilayer to a finite value in solution. The magnitude of the charge separation was tuned to match the experimental transmembrane potential (300 mV). This gave a value of ~0.6 Debye per lipid normal to the bilayer (Fig. S4). For a 16 nm diameter domain, we found that for various monovalent salt concentrations the transverse potential in the headgroup region falls off exponentially upon moving radially outward from the edge of the domain. Even for the case of no salt (which matches the experimental conditions) we found an exponential decay length of no more than 4 nm (Fig. S5). This analysis shows that the use of a long range dipole-dipole term in the energy functional might be justified only for very small nanodomains. We are currently studying other possible long range competing interactions to explain the modulated phase shapes and sizes, such as domain curvature interacting with bilayer fluctuations, or an intrinsic property of the Lo phase that is favorable for smaller domains.

REFERENCES

1. Morales-Penningston N.F, J. Wu, E.R. Farkas, S.L. Goh, T.M. Konyakhina, J.Y. Zheng, W.W. Webb, and G.W. Feigenson. 2010. GUV Preparation and Imaging: Minimizing Artifacts. *Biochim. Biophys. Acta.* 1798:1324-1332.
2. M.I. Angelova, S. Soléau, P. Méléard, J.F. Faucon and P. Bothorel. 1992. Preparation of giant vesicles by external AC fields. Kinetics and application. *Prog. Colloid Polym. Sci.* 89:127-131
3. Akashi, K., H. Miyata, H. Itoh, and K. Kinosita, Jr. 1996. Preparation of giant liposomes in physiological conditions and their characterization under an optical microscope. *Biophys. J* 71:3242-3250.
4. Seul, M. and D. Andelman. 1995. Domain Shapes and Patterns: The Phenomenology of Modulated Phases. *Science*. 267:476-483.
5. Travesset, A. 2006. Effect of dipolar moments in domain sizes of lipid bilayers and monolayers. *J..Chem Phys.*. 125: 084905.

TABLE S1 Percentage of GUVs having the observed morphologies

ρ	N GUV	% macroscopic	% modulated	% uniform
10	60	2	31	67
15	82	15	63	22
20	89	22	70	8
25	88	23	74	3
30	66	80	20	0

TABLE S1 shows the count distribution of three main GUV morphologies (macroscopic round domains; modulated domains; uniform) observed from ρ = 10-30, at χ_{DSPC} = 0.45 and χ_{chol} = 0.25.

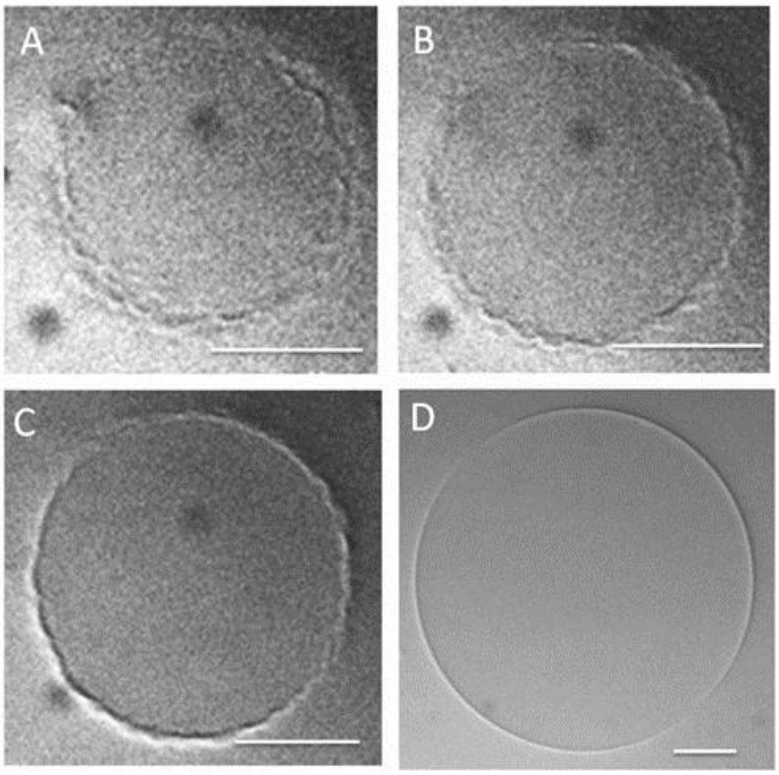

FIGURE S1. DIC images of a GUV without probe C12:0-DiI show scalloped edges at ρ =20% (A-C) compared to a probe-free, uniform GUV (D). (A-C) shows the same GUV at different planes of a z-stack. Compositions DSPC/DOPC/POPC/chol: (A-C) 0.45/0.06/0.24/0.25; (D) 0.45/0.03/0.27/0.25. Scale bars 10 μm, temperature 23°C.

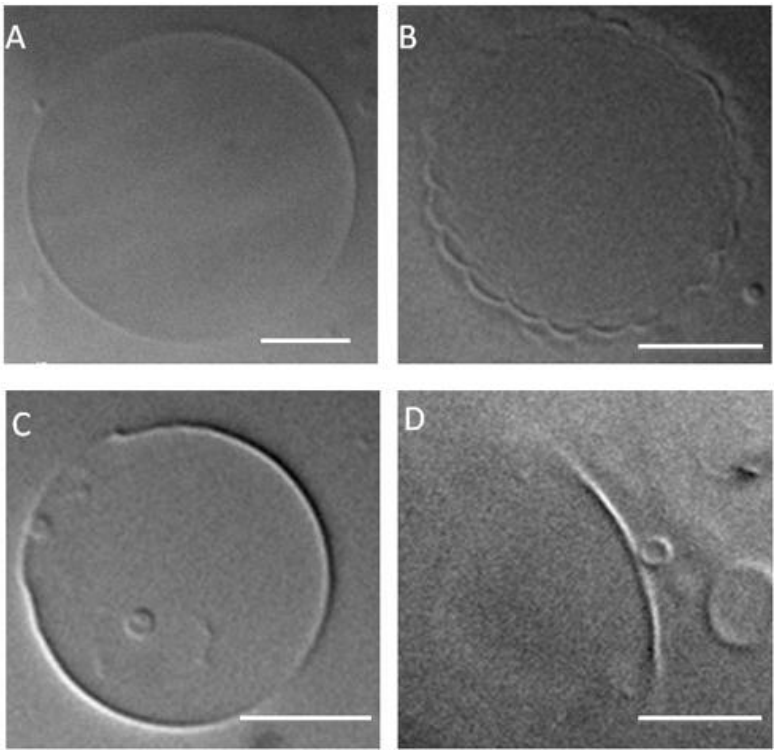

FIGURE S2. GUV morphologies imaged with DIC. (A) uniform, featureless with smooth edges; (B) scalloped edges pattern; (C) budding vesicle; (D) border of Lo + Ld macroscopic phases. Compositions of DSPC/DOPC/POPC/chol: (A) 0.45/0.015/0.285/0.25; (B) 0.45/0.045/0.255/0.25; (C) 0.45/0.09/0.21/0.25; (D) 0.45/0.30/0/0.25. Scale bars 10 μm, temperature 23°C.

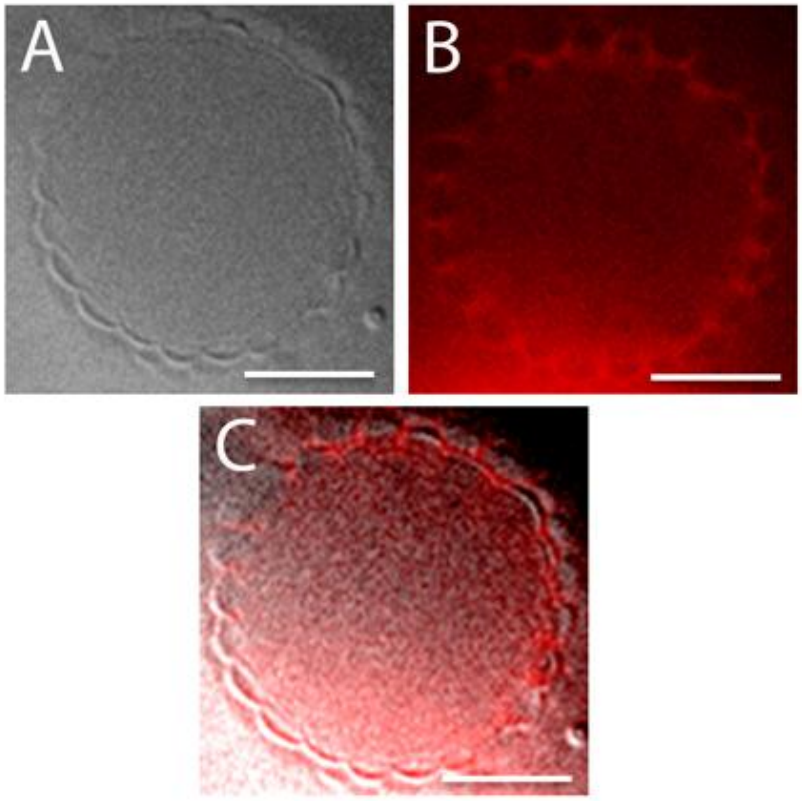

FIGURE S3. Complementarity of fluorescence and DIC images for a GUV with honeycomb pattern at DSPC/DOPC/POPC/chol = 0.45/0.045/0.255/0.25. (A) DIC; (B) fluorescence image, C12:0-DiI at 0.02 mol%; (C) superimposition of DIC and fluorescence images. Scale bars 10 µm, temperature 23°C.

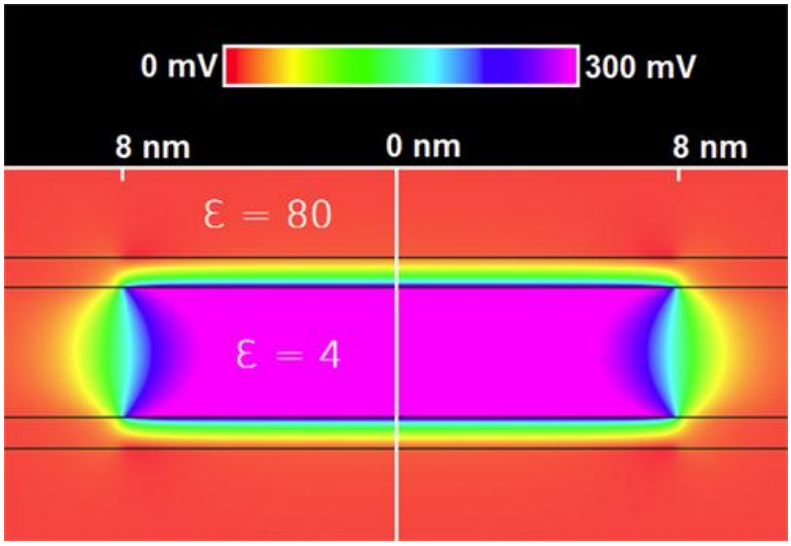

FIGURE S4. Cross section of the bilayer showing the electrostatic potential obtained by solving Eq. S5 everywhere inside a 16 nm circular domain with a Debye length of 1 nm in solution.

.

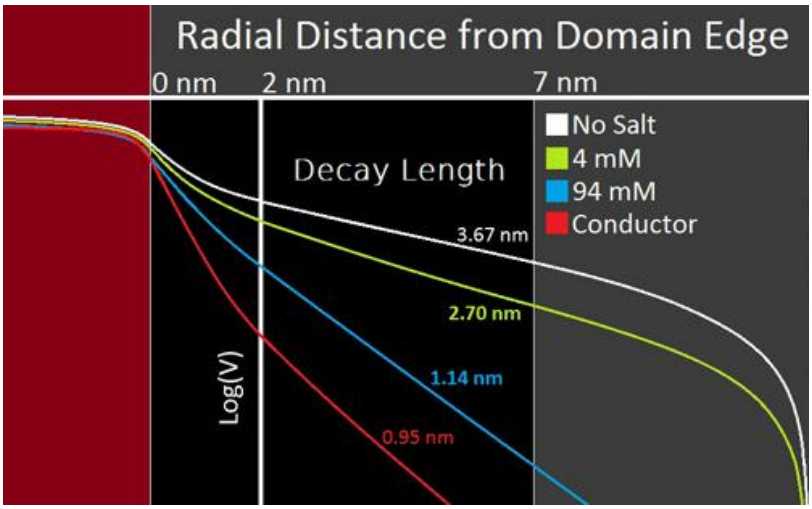

FIGURE S5. Log plot of the potential in the headgroup region moving radially outward from the edge of the domain (red) for various salt concentrations. Decay lengths are shown next to each curve.